

# Characteristics of tin nitride thin-film negative electrode for thin-film microbattery

K.S. Park<sup>a,\*</sup>, Y.J. Park<sup>b</sup>, M.K. Kim<sup>a</sup>, J.T. Son<sup>a</sup>, H.G. Kim<sup>a</sup>, S.J. Kim<sup>c</sup>

<sup>a</sup>Department of Materials Science and Engineering, Korea Advanced Institute of Science and Technology, Taejon 305-701, South Korea

<sup>b</sup>Battery Technology Team, Telecommunication Basic Research Laboratory, Electronics and Telecommunications Research Institute (ETRI), 161 Kajong-Dong, Yusong-Gu, Taejon 305-350, South Korea

<sup>c</sup>Department of Electrical Engineering, Donghae University, 119 Jiheung-Dong, Donghae, Kangwon-Do, South Korea

Received 7 March 2001; accepted 27 May 2001

## Abstract

Tin nitride is a relatively unknown compound. In this study, the tin nitride thin film is examined as a negative electrode for a thin-film microbattery. Reactive rf magnetron sputtering is used for deposition of films with varying deposition temperature. The charge–discharge properties of thin films deposited at room temperature, 100 and 200°C are found to be satisfactory. As the irreversible capacity fraction increases, rechargeability is improved. Finally, it is suggested that the electrochemical characteristics of tin nitride are similar to those of the tin oxide system. The charge–discharge characteristics are investigated in several ways. © 2001 Elsevier Science B.V. All rights reserved.

**Keywords:** Tin nitride; Thin film; Microbattery; Lithium battery; Negative electrode; Anode

## 1. Introduction

Advances in the microelectronics industry have reduced the current and power requirements of electronic devices. Therefore, thin-film solid-state microbatteries can be employed as power sources for devices such as smart cards, CMOS-based integrated circuits (IC), and microdevices [1].

Lithium metal has generally been used for the negative electrode material in thin-film microbatteries. When a microbattery is integrated into an IC, it must endure temperatures as high as 250–260°C for 10 min. Lithium metal is not stable at a high process temperature due to its low melting point (181°C), and in air due to its high reactivity [2,3]. To solve these problems, many researchers have searched for alternative negative electrode materials such as tin-based oxides.

The proposed charge–discharge mechanism of tin oxide in the lithium secondary battery is alloying/dealloying [4,5]. When lithium is inserted into the tin oxide during the first discharge reaction, it decomposes and a thermodynamically stable amorphous Li<sub>2</sub>O matrix forms. Then, lithium and metallic tin form a Li–Sn alloy. During the charge reaction, the Li–Sn alloy decomposes into lithium and metallic tin. The Li<sub>2</sub>O remains stable, however, so this

causes the problem of irreversible capacity loss. Previous work has suggested that the irreversibly formed Li<sub>2</sub>O can absorb the stress produced by Li–Sn alloying/dealloying which is accompanied by a large volume change, and can sustain electrical contact between the tin particles [4,6]. Thus, if the Li<sub>2</sub>O content is low, it may also impair electrode properties.

Tin oxide shows the best electrochemical properties among the oxides of the metals of Groups III–V. On the other hand, it also displays a large irreversible capacity loss during the first discharge reaction [6]. To overcome this problem, a tin nitride thin-film negative electrode is examined in this paper.

Tin nitride is a relatively unknown compound. In 1908, Fischer and Iliovichi reported [7,8] that the stoichiometry of tin nitride is Sn<sub>3</sub>N<sub>4</sub>. It is non-toxic and stable at room temperature and in air [9]. To date, little work has been carried out on microbatteries which use this material as a negative electrode.

## 2. Experimental

The deposition of thin films of tin nitride on Pt/Ti/SiO<sub>2</sub>/Si substrates was carried out by means of a reactive rf magnetron sputtering system, using a 4 in. diameter target of metallic tin (99.999% pure, Cerac). The base pressure in

\* Corresponding author. Tel.: +82-42-869-4152; fax: +82-42-869-8650.  
E-mail address: gappa@kaist.ac.kr (K.S. Park).

the chamber was set below  $5 \times 10^{-6}$  Torr during heating to the deposition temperature, and the working pressure was controlled to 30 mTorr in the Ar/N<sub>2</sub> (5:5 sccm) gas mixture atmosphere. The rf power density was  $0.6 \text{ W cm}^{-2}$  to obtain the plasma. The experimental variable was the deposition temperature over the range room temperature to 300°C. The thicknesses of the thin films was fixed to 1000 Å in order to eliminate any effect from this thickness.

### 2.1. Characterization of the basic properties of thin films

The surface microstructure was observed by means of scanning electron microscope (SEM) with a Philips XL30 SFEG instrument and X-ray diffraction (Rigaku, Cu K $\alpha$  radiation) was used to examine the crystallinity changes caused by variation of the deposition temperature. Quantitative analysis was carried out by WDS (wavelength-dispersive spectroscopy) and the result showed that the composition was approximately Sn:N = 3:4. The stylus ( $\alpha$ -step 500, TENCOR) was used to calculate the volumetric capacity. The chemical state change of the tin in the tin nitride thin film after the charge–discharge process was analyzed by X-ray photoelectron spectroscopy (XPS).

### 2.2. Characterization of electrochemical properties of thin films

For electrochemical measurements, the tin nitride thin film was placed in an open beaker cell, which contained 1 M LiClO<sub>4</sub> in propylene carbonate (PC), in an argon atmosphere glove box. Metallic lithium foil (99.99% pure, Foote Mineral Co.) was used for the counter and reference electrodes while the tin nitride thin film was used as the working electrode. The charge–discharge tests were controlled with a EG&G Multi-Potentiostat/Galvanostat system (MPS, model 200). The charge–discharge characteristics and rechargeabilities of the cell were analyzed by performing a cycle test at the same current density ( $300 \mu\text{A cm}^{-2}$ ) in the voltage range 1.1–0.1 V. To obtain the cyclic voltammogram, the scan rate was set at  $0.1 \text{ mV s}^{-1}$  in the same experimental system and voltage range.

## 3. Results and discussion

### 3.1. Structure determination of tin nitride thin films

The X-ray diffraction patterns of tin nitride thin films deposited at room temperature, 100, 200 and 300°C are given in Fig. 1. Peaks marked with S correspond to the substrate silicon wafer and platinum layer. The intensity of the SnN<sub>x</sub>(2 0 0) peak is very weak while the Si(2 0 0) substrate peak at around 33° shows a somewhat broad shape at its bottom. In the case of tin nitride, (1 0 1) and (0 0 2) peaks exist at 32.7 and 34.2°, respectively [10]. These seem to influence the broad shape of the Si(2 0 0) peak. Thus, it is

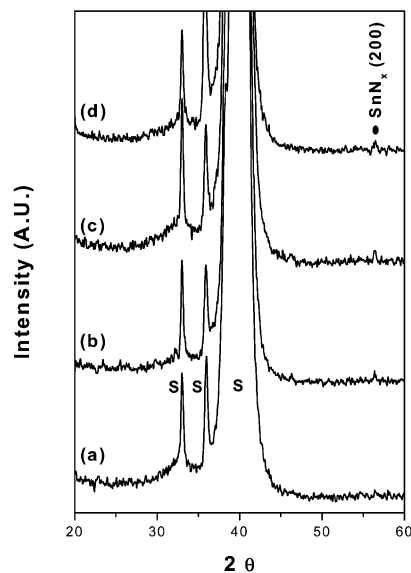


Fig. 1. X-ray diffraction patterns of tin nitride thin films deposited at (a) room temperature; (b) 100°C; (c) 200°C; (d) 300°C. Peaks marked with S correspond to the substrate silicon wafer and platinum layer.

hard to explain the change in crystallinity and orientation from this X-ray diffraction data. From the peak intensity, however, it can be inferred that the thin films have poor crystallinity.

The surface microstructures of thin films deposited at room temperature, 100, 200 and 300°C were observed by SEM at a magnitude of 150,000 and are presented in Fig. 2. It is seen that all the thin films have a very small and uniform grain-size distribution. This can be explained by the very weak X-ray diffraction peak intensity of the tin nitride. It is also found that the grain size is slightly increased and the microstructure becomes denser as the deposition temperature is raised.

### 3.2. The electrochemical properties of tin nitride thin films

The charge–discharge characteristics of the tin nitride thin film deposited at room temperature are presented in Fig. 3. There is a plateau at about 1.1 V in the first discharge reaction. The second discharge capacity is decreased to 40% of its first discharge capacity. After the first cycle, the reversible charge–discharge reactions are maintained.

The variation in discharge capacity for 100 cycles with respect to the deposition temperature is given in Fig. 4. The irreversible capacity losses are about 30–60% of the initial first discharge capacity after the first discharge reaction. As the deposition temperature increases, the discharge capacity increases and the reason for this tendency is perhaps that the thin film densifies and leads to the abundant production of active material. The rechargeability degrades, however, for the reason given below. All the discharge capacities are sufficiently large to utilize the tin nitride thin film negative electrode for the thin-film microbattery.

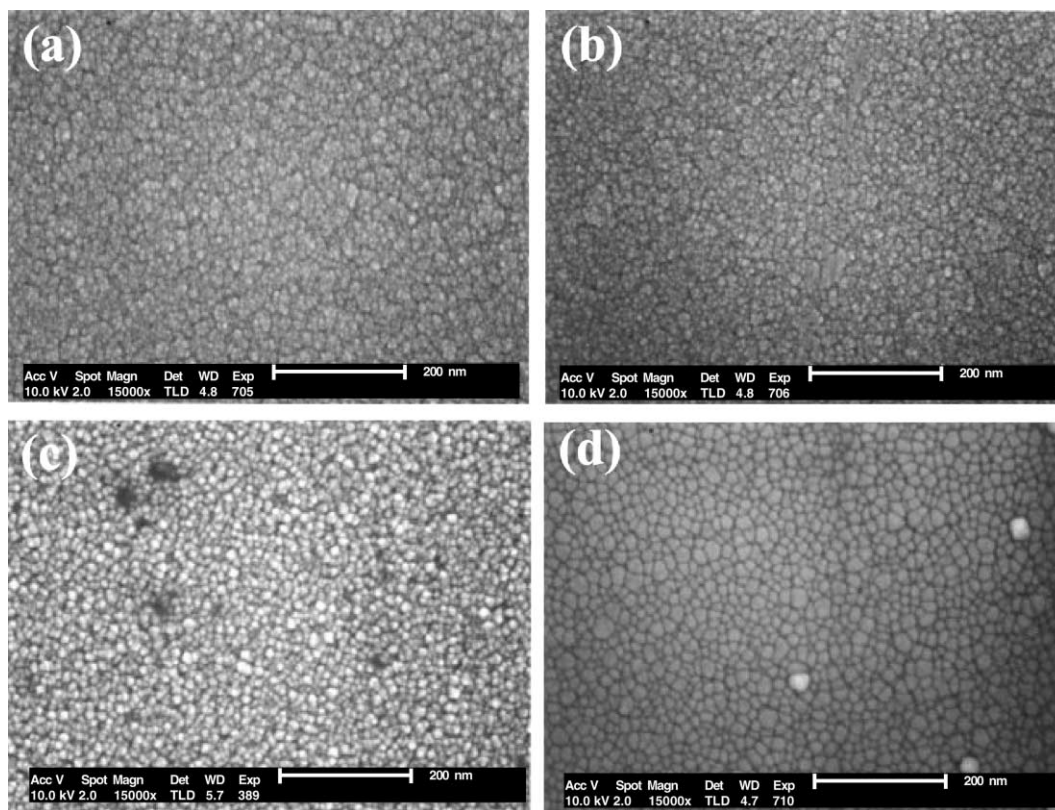


Fig. 2. SEM images (150,000×) of tin nitride thin films deposited at (a) room temperature; (b) 100°C; (c) 200°C; (d) 300°C. It is seen that all the thin films have a very small and uniform grain-size distribution.

In the case of tin oxide, the  $\text{Li}_2\text{O}$  which is irreversibly formed during the first discharge reaction can reduce the stress produced by alloying/dealloying of the Li–Sn. Thus, if the  $\text{Li}_2\text{O}$  content is large, the rechargeability of the cell is improved. The irreversible capacity loss fraction with respect to the initial discharge capacity is shown in Fig. 5. As the deposition temperature increases, the irreversible capacity loss fraction decreases. Compared with the results

given in Fig. 4, as the irreversible capacity loss fraction increases, the rechargeability of the cell is improved. Thus, it appears that there is some relation between the degree of irreversible capacity loss and the cycle properties of the tin nitride system.

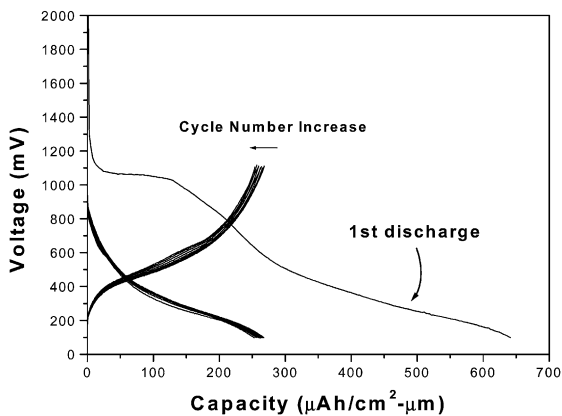


Fig. 3. Charge–discharge curves of tin nitride thin films deposited at room temperature for 100 cycles under  $300 \mu\text{A cm}^{-2}$ .

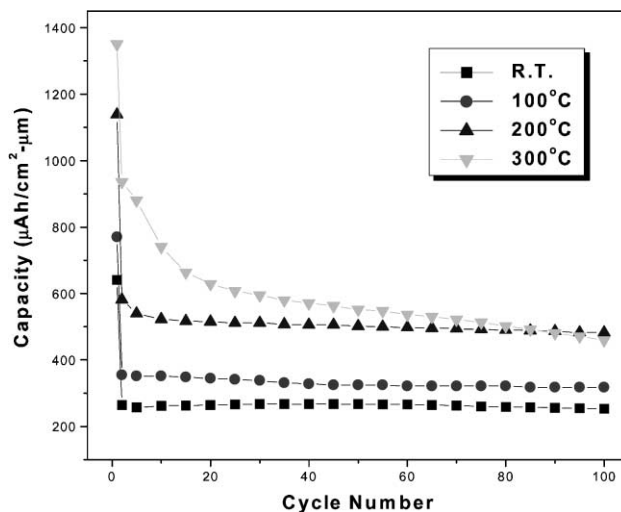


Fig. 4. Discharge capacity variation for 100 cycles. As deposition temperature increases, discharge capacity increases but rechargeability degrades.

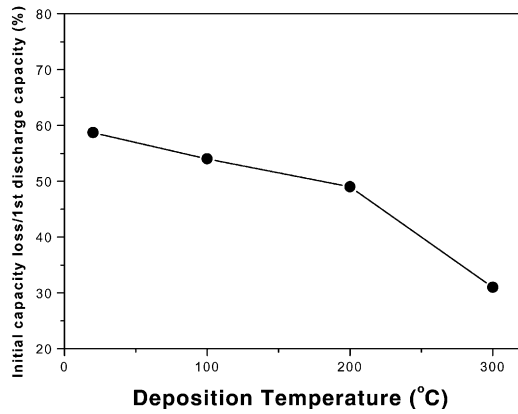


Fig. 5. Variation of irreversible capacity loss fraction with deposition temperature. As deposition temperature increases, irreversible capacity loss fraction decreases.

### 3.3. Analysis of charge–discharge characteristics

Cyclic voltammograms for the thin film deposited at 200°C are given in Fig. 6. The voltage range is from 1.1 to 0.1 V, and the scan rate is 0.1 mV s<sup>-1</sup>. A broad peak occurs at around 0.9 V in the first discharge reaction, but disappears during further discharge reactions. This confirms that there is an irreversible reaction in the first discharge reaction as indicated by the cycle properties given in Fig. 3.

Ex situ X-ray diffraction of the thin film deposited at 200°C was taken before and after the charge–discharge tests and the results are given in Fig. 7. A SnN<sub>x</sub>(2 0 0) peak was not found after the first cycle, and the Si(2 0 0) substrate peak at around 33° no longer has a broad shape at its bottom. A weak metallic Sn(2 0 0) peak is observed after the first cycle and a metallic Sn(2 0 0), (1 0 1) peak after the hundredth cycle. This suggests that the irreversible reaction on the first discharge is related to the decomposition of the tin

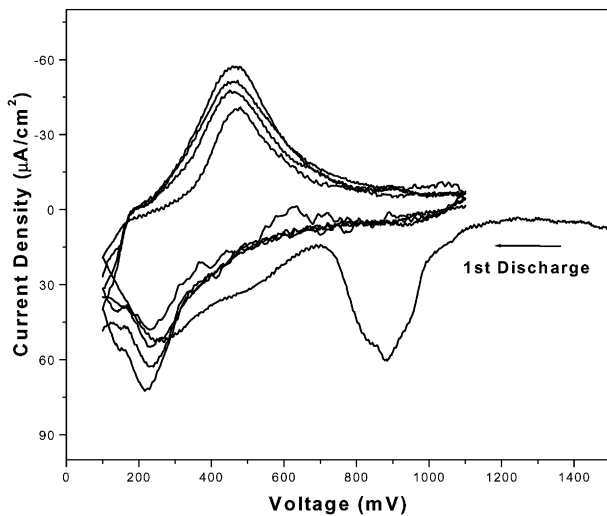


Fig. 6. Cyclic voltammograms (0.1 mV s<sup>-1</sup>) of thin films deposited at 200°C for first 4.5 cycles.

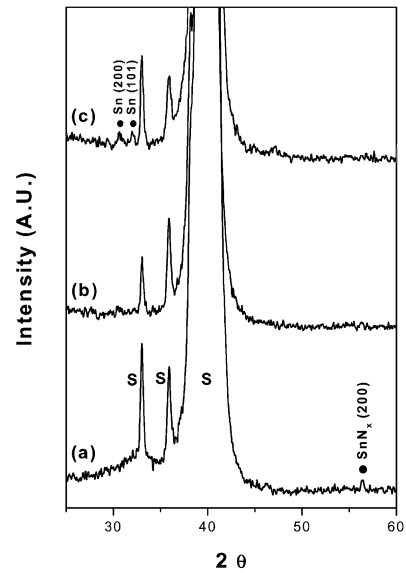


Fig. 7. Ex situ X-ray diffraction patterns: (a) before first discharge; (b) after first cycle; (c) after 100th cycle. No SnN<sub>x</sub>(2 0 0) peak is found after first cycle, and a metallic tin peak is observed.

nitride and after this only the metallic tin takes part in the charge–discharge reaction.

X-ray photoelectron spectroscopy (XPS) studies were undertaken to analyze the change in the chemical state of the tin during the first cycle. The peak shift caused by the charging effect is compensated with C 1s peak (284.6 eV) and the result is given in Fig. 8. The binding energy (BE) of the Sn 3d<sub>5/2</sub> peak before cycling is about 486 eV and changes to 485.2 eV. From this experimental result, two possible explanations can be advanced. First, a transition of the chemical state of tin from a compound state to a metallic state has occurred and second, the nitrogen which bound to the tin initially exists as another form after the first cycle.

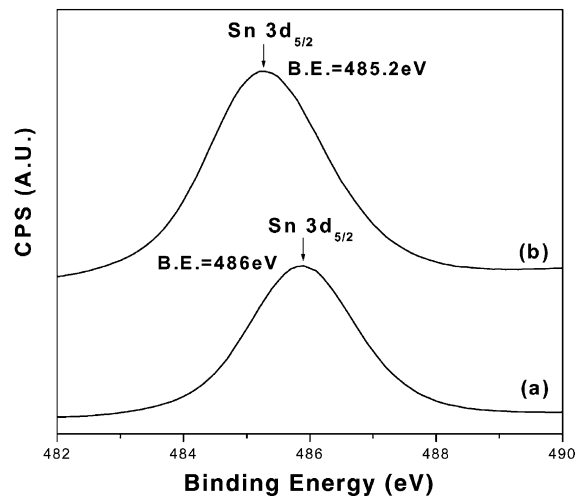


Fig. 8. XPS spectra of Sn 3d<sub>5/2</sub> of thin films deposited at 200°C, 30 mTorr (a) before and (b) after first cycle.

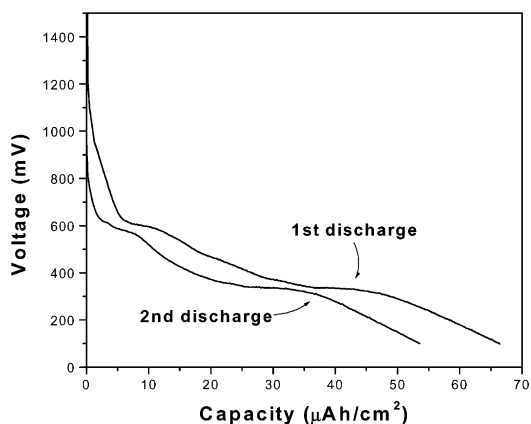


Fig. 9. Charge–discharge curves of metallic tin thin film deposited at room temperature.

To analyze the charge–discharge characteristics, tests were performed on thin films of metallic tin, see Fig. 9. In this case, the thickness of the thin film was of no concern, attention was focused on the electrochemical properties. The thin film was deposited at room temperature and in an argon atmosphere. A plateau similar to that found at around 0.8–1.1 V for the tin nitride thin films is not present. Also, as it has been reported [11,12] that the equilibrium potential between tin and lithium is under 0.7 V, comparison with the ex situ XRD result suggests that the plateau of the tin nitride is formed by reaction between lithium and nitrogen (e.g. compound formation). This reaction product may exist irreversibly during the charge–discharge reaction.

In summary, ex situ X-ray diffraction results show that tin nitride decomposes during the first cycle, and that this is related to the irreversible capacity loss. It is further deduced that only the metallic tin takes part in the charge–discharge reaction after the first cycle, and the XPS spectrum confirms that the chemical state of tin is changed to a metallic state during the first cycle. From comparison with the charge–discharge properties of the thin film of metallic tin, it is concluded that the plateau of the tin nitride thin films in the first discharge reaction is formed by electrochemical reaction between lithium and nitrogen. Moreover, tin oxide exhibits the same voltage profile after the first cycle [13]. Therefore, it can be inferred that the charge–discharge characteristics of tin nitride thin films are caused by reaction between lithium and nitrogen followed by alloying/dealloying of Li–Sn.

#### 4. Conclusions

Thin films of tin nitride have been deposited by reactive rf magnetron sputtering. As the deposition temperature increases, the thin film becomes denser. The electrochemical properties of thin films deposited at room temperature, 100 and 200°C are good enough to utilize, but the properties degrade for the film deposited at 300°C. As found with the tin oxide system, rechargeability is improved when the irreversible capacity loss fraction increases.

It is suggested that the electrochemical properties of the tin nitride are associated with alloying/dealloying of Li–Sn. The origin of irreversible capacity loss can be understood by the reaction between nitrogen and the inserted lithium, and after the first cycle only metallic tin takes part in the electrochemical reaction.

The merits of tin nitride thin-film negative electrodes are as follows. Tin nitride has sufficient capacity for application in thin-film microbatteries and compared with the tin oxide reported previously [13], its initial capacity loss is smaller. In addition, the tin nitride displays good cycle-life after the initial discharge reaction.

#### References

- [1] Y.J. Park, J.G. Kim, M.K. Kim, H.T. Chung, W.S. Um, M.H. Kim, H.G. Kim, *J. Power Sources* 76 (1998) 41–47.
- [2] J.B. Bates, N.J. Dudney, B. Neudecker, A. Ueda, C.D. Evans, in: *Proceedings of the 12th International Conference on Solid State Ionics*, 1999, p. A-KE-03.
- [3] P. Birke, S. Doring, W. Weppner, in: *Proceedings of the 11th International Conference on Solid State Ionics*, 1997, p. 70.
- [4] I.A. Courtney, J.R. Dahn, *J. Electrochem. Soc.* 144 (1997) 2045–2052.
- [5] W. Liu, X. Huang, Z. Wang, H. Li, L. Chen, *J. Electrochem. Soc.* 145 (1998) 59–62.
- [6] T. Brousse, R. Retoux, U. Herterich, D.M. Schleich, *J. Electrochem. Soc.* 145 (1998) 1–4.
- [7] F. Fischer, G. Iliovichi, *Ber. Deut. Chem. Ges.* 41 (1908) 3802.
- [8] F. Fischer, G. Iliovichi, *Ber. Deut. Chem. Ges.* 42 (1909) 527.
- [9] T. Maruyama, T. Morishita, *Appl. Phys. Lett.* 69 (1996) 890–891.
- [10] R.S. Lima, P.H. Dionisio, W.H. Schreiner, C. Achete, *Solid State Commun.* 79 (1991) 395–398.
- [11] R.A. Huggins, *J. Power Sources* 26 (1989) 109–120.
- [12] J. Wang, I.D. Raistrick, R.A. Huggins, *J. Electrochem. Soc.* 133 (1986) 457.
- [13] Y.J. Park, K.S. Park, J.G. Kim, M.K. Kim, H.G. Kim, H.T. Chung, *J. Power Sources* 88 (2000) 250–254.